SCIENCE CHINA Information Sciences



• RESEARCH PAPER •

December 2025, Vol. 68, Iss. 12, 220306:1–220306:12 https://doi.org/10.1007/s11432-025-4638-7

Special Topic: Terahertz Communications for 6G and Beyond: How Far Are We?

330 GHz antistatic compact vertical interconnect IQ transceiver for 6G communication

Zhongqian NIU¹, Qianli YIN¹, Bo ZHANG¹*, Zhao QI¹, Yinian FENG¹, Yong FAN² & Zhi CHEN²

¹School of Electronic Science and Engineering, University of Electronic Science and Technology of China,

Chengdu 610054, China

²National Key Laboratory of Science and Technology on Communications,

University of Electronic Science and Technology of China, Chengdu 610054, China

Received 29 April 2025/Revised 17 August 2025/Accepted 20 October 2025/Published online 14 November 2025

Abstract This paper introduces a compact 330 GHz antistatic IQ transceiver designed for high-speed wireless communication. To maximize space efficiency, the transceiver's internal cavity is divided into two functional layers: a THz layer and an IF (intermediate frequency) layer. The THz layer is implemented on a quartz substrate and two Schottky diode-based subharmonic mixers along with a pair of compact, arch-shaped 90-degree hybrid couplers. The IF layer houses two low-noise amplifiers and an additional 90-degree hybrid coupler. The entire system operates in an IQ balanced mixer configuration, enabling effective image rejection and single-sideband (SSB) signal transmission. Experimental measurements show a best-case SSB receiver conversion loss of 8 dB at 330 GHz and image rejection exceeding 18 dB across the 305–355 GHz frequency range. Despite its advanced performance, the transceiver maintains a remarkably compact footprint of just 20 mm × 22 mm. A key feature of this design is its antistatic capability: the integrated chipset can withstand up to 8000 V of static discharge, providing robust protection for the sensitive Schottky diode-based components. Based on this IQ mixer, a high-speed communication experiment was successfully demonstrated, achieving a data rate of 40 Gbps using 16QAM modulation, offering a critical building block for future 6G communication technologies.

Keywords THz solid state circuit, IQ transceiver, vertical interconnect, compact circuits, 6G communication

Citation Niu Z Q, Yin Q L, Zhang B, et al. 330 GHz antistatic compact vertical interconnect IQ transceiver for 6G communication. Sci China Inf Sci, 2025, 68(12): 220306, https://doi.org/10.1007/s11432-025-4638-7

1 Introduction

Terahertz communication technology has emerged as a vital focus in the evolution of 6G high-speed wireless systems [1–3]. With the continuous advancement of wireless technologies, the limited availability of conventional frequency spectrum has become increasingly problematic, driving the need to explore new spectral domains such as the terahertz band. This frequency range merges the strengths of microwave and optical communications, offering high data transmission rates, large information capacity, strong directionality, and improved security. The terahertz band provides a wealth of untapped spectrum resources, effectively overcoming bandwidth constraints and enabling the transmission of high-volume data to meet growing demands for ultra-fast communication [4–6]. Additionally, it supports enhanced system security, directional transmission, and the potential for compact, miniaturized device designs [7–9].

In terahertz communication systems, terahertz IQ mixers play a crucial role in selecting useful signals and suppressing mirror frequency signals, making them highly effective in combating interference. These IQ mixers typically utilize the subharmonic mixing method, consisting of two mixers and several couplers. The performance and consistency of the mixer directly influence the IQ mixer's overall performance.

The IQ mixer generates two IF signals (I-channel and Q-channel) with orthogonal phases and equal amplitudes. In continuous wave Doppler radar systems employing the zero IF architecture, studying the relative phase relationship between these two IF signals can accurately determine the motion trajectory of objects [10]. In the FMCW radar leakage cancellation system, the transmitted signal serves as the local oscillator signal for the IQ mixer, while the leakage signal is an RF signal. By adjusting the output of the

 $[\]hbox{$*$ Corresponding author (email: zhangbouestc@yeah.net)}\\$

two IF signals, a control signal is provided to the vector modulator, enabling the cancellation of unwanted signals [11]. In instrument measurement applications, the IQ mixer is connected in series with the tested component, allowing the extraction of amplitude and phase information from the two intermediate frequency signals [12]. Moreover, in communication systems, IQ mixers facilitate SSB transmission, enabling I/Q modulation of baseband signals at zero intermediate frequency. This capability proves highly valuable in achieving efficient communication processes.

Terahertz IQ mixers hold significant importance, but their complex circuit structure leads to larger volumes and intricate connections in existing IQ mixers [13–17]. Typically, IF circuits and terahertz circuits are treated as independent components, linked together through coaxial lines. This arrangement arises due to the usage of waveguides for transmission in terahertz circuits. However, manufacturing rectangular waveguide structures on pure metal lacks processing flexibility and poses challenges in dealing with corner and torsion waveguide structures. As a result, traditional terahertz circuits are mostly single-layer circuits, making vertical interconnection difficult to achieve. Despite the terahertz circuit's small size, usually in the millimeter range, the waveguide flange adheres to an international standard size, with a single circuit flange measuring about 2 cm. Unfortunately, many existing terahertz circuits contain only one circuit in a cavity, leading to significant internal space wastage and contributing to the bulky size of the current terahertz front-end.

Additionally, electrostatic protection poses a significant concern in terahertz Schottky diode-based circuits. The Schottky mixing diode operates at low carrying voltage and power, and its direct connection to the IF microstrip line allows external static electricity to reach the diode through the conductor of the IF SMA interface, potentially resulting in diode burnout. Human body static electricity can easily cause damage to Schottky mixer diodes, prompting internationally renowned terahertz circuit manufacturers like Virginia Diodes Inc. (VDI) or ACST GmbH (ACST) to emphasize electrostatic protection measures in their product data sheets to prevent circuit damage. A common solution involves wearing an electrostatic bracelet or using an IF connection isolator to mitigate the risk of damage. However, these protective measures increase the complexity of circuit debugging and lead to additional circuit connection losses.

In summary, to safeguard terahertz mixers from static electricity damage, achieve mirror frequency suppression function, and advance terahertz communication technology, the urgent need is to develop miniaturized and high-performance terahertz IQ mixers.

This paper introduces a 330 GHz antistatic compact vertical interconnect IQ transceiver to address these challenges. The IQ transceiver comprises two layers: the THz layer and the IF layer. The THz layer includes two 330 GHz subharmonic mixers, a 165 GHz and a 330 GHz 90° arch-shaped hybrid couplers. Additionally, an anti-static chip is placed in the terahertz layer, directly connected to the IF ports of the subharmonic mixers, preventing external static electricity from entering the terahertz circuit. The IF layer consists of two 0.1–10 GHz low noise amplifiers and a 2–8 GHz 90-degree broadband low amplitude and low phase imbalance hybrid. The vertical interconnection between the THz and IF layers is achieved through SMP connectors, offering advantages such as low loss, small size, high operating frequency, and fast connection and separation. This design allows independent measurement of each circuit layer, optimizing the overall IQ mixer's performance.

Owing to the compact circuit layout and vertical interconnect architecture, the transceiver achieves an overall size of just $20~\text{mm} \times 20~\text{mm} \times 22~\text{mm}$. Measurement results demonstrate that with a LO drive power of 10~mW, the conversion loss for both the I and Q channels remains below 10~dB across a 40~GHz bandwidth centered at 330~GHz. The typical mirror suppression ratio is approximately 18~dB. Communication experiments have validated the capability for single-channel transmission at 40~Gbps. The IQ mixer is designed for prospective 6G applications, enabling high-speed, real-time SSB anti-interference communication as well as IQ-modulated signal transmission.

2 Transceiver architecture and circuits

In wireless communication systems, the integrated development of transceivers faces challenges due to image frequency and image suppression issues. However, IQ mixers offer a solution, enabling progress towards achieving low-power consumption and cost-effective communication systems. The Hartley structure, known for its simplicity, has become the most commonly used circuit topology for mirror suppression mixers [18]. In this structure, the RF signal and LO signal are fed into the mixer through separate channels, with a relative phase difference of 90° between them. After mixing, the signal passes through a

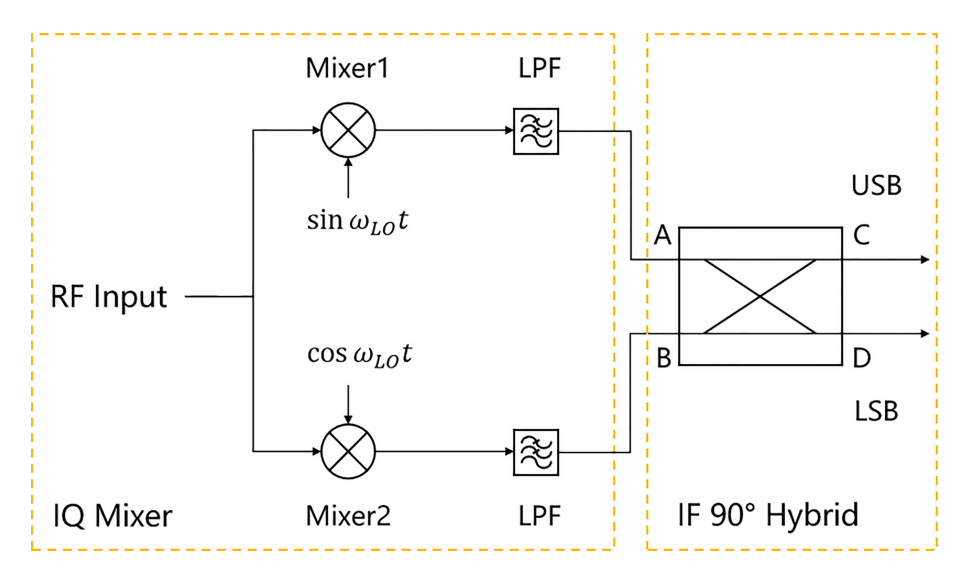


Figure 1 (Color online) The basic structure of the image rejection IQ mixer.

low-pass filter, and the IF signal in the upper channel undergoes a 90° phase transformation process. Subsequently, both channels are directed to an IF 90° hybrid, as illustrated in Figure 1. At port C, only the upper sideband signal exists, while at port D, only the lower sideband signal is present. By connecting a matching load to the output port of the desired sideband, mirror frequency suppression is achieved accordingly.

An IQ mixer is typically composed of two identical mixing units and a phase-shifting network. Its characteristic is that the two IF signals at the output have consistent amplitude values and orthogonal phase differences. When the RF input signal frequency is lower than the LO, the IQ mixer exhibits a delay characteristic between the two IF signals. Conversely, it shows a leading characteristic when the RF input signal frequency is higher than the LO frequency. Based on these two characteristics, the mixer is widely used in radar, communication, and measurement systems.

2.1 330 GHz IQ mixer derivation and topology

According to the Hartley structure, the IQ mixer offers various options for its circuit topology as long as the relative phase difference between the RF signal and the LO signal is 90° during mixing. Typically, IQ fundamental mixers utilize a phase-shifted network with a 90° phase shift on either the local oscillator or RF side. However, in the terahertz frequency band, subharmonic mixers are preferred due to their simplicity, good noise performance, and low LO driving requirements. Due to the nature of subharmonic mixers, the relative phase shift of the LO signal will be doubled, resulting in only half of the phase difference required for the LO port. Because of different phase shift networks, there are performance differences between the two mixers of the IQ mixer. Therefore, to minimize the imbalance of the amplitude and phase of the two IF outputs, it becomes necessary to analyze the advantages and disadvantages of each topology structure before selecting a suitable subharmonic IQ mixer circuit. For subharmonic IQ mixers, there are typically two circuit topologies, as illustrated in Figure 2 [19].

If a 45-degree phase-shifted hybrid structure is employed, as shown in Figure 2(a), it offers the advantage of allowing the RF end to directly utilize a simple power divider. In the low-frequency band, the Wilkinson power divider can easily match with the mixer, resulting in effective suppression of mirror frequencies. However, when operating in the terahertz frequency band, power divider circuits based on Y-junction or balanced E-plane probe structures suffer from poor isolation. This deficiency leads to significant imbalances and ripples in the receiving system [14], making this circuit topology unsuitable for terahertz applications.

Branch waveguide hybrid couplers offer several advantages, including broadband operation, low amplitude phase imbalance, high isolation, low loss, and a simple structure. These characteristics make them highly suitable for subharmonic IQ mixers, as they fulfill the 90° phase shift requirements. Additionally, the 3 dB hybrid coupler, being a four-port matching circuit, not only provides high isolation between two subharmonic mixers but also reduces standing wave coefficients at the RF and LO ports, thereby enhancing the IQ mixer's overall performance.

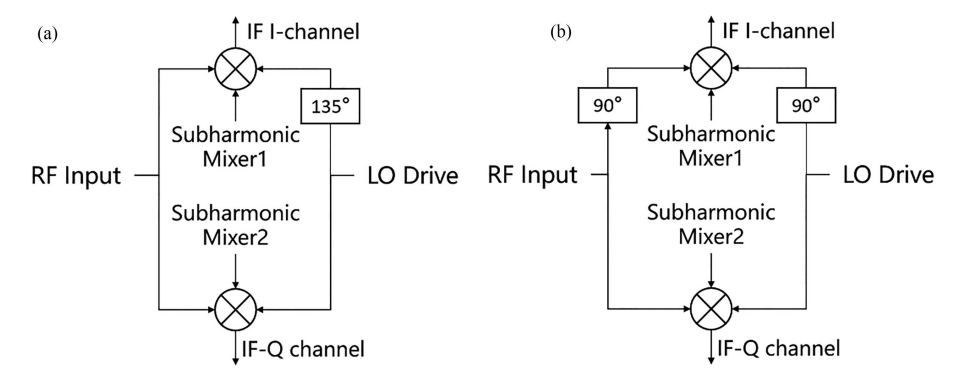


Figure 2 Commonly used even-harmonic IQ mixer topologies are as follows: (a) LO 45-degree phase shift and (b) RF 90-degree phase shift.

The LO signal is split into two channels with identical amplitude and orthogonal phase using a 3 dB branch waveguide hybrid coupler. These channels provide driving power to the I and Q subharmonic mixers, ensuring the proper functioning of the mixer. Due to the subharmonic mixing structure, the phase of the LO signal doubles during mixing. As a result, the mixer circuit generates two IF signals (I-channel and Q-channel) with the same amplitude but a 90° phase difference. These two signals are then directed to an IF hybrid to achieve sideband separation. The theoretical derivation is as follows.

Assuming subharmonic mixer I as a reference, the phase difference between subharmonic mixer Q and subharmonic mixer I is represented by $\Delta \psi$. The output IF signal current of mixer I is as follows:

$$i_{\text{if-I}}(t) = \sum_{m=-\infty}^{m=+\infty} \sum_{n=-\infty}^{n=+\infty} \left[I_{m,n} e^{j(m\omega_L + n\omega_s)t} \left(1 - e^{j(m+n)\pi} \right) \right], \tag{1}$$

where m stands for the harmonic order of the LO signal, and n stands for the harmonic order of the RF signal. For subharmonic mixers, $m = 2, n = \pm 1$, then

$$i_{\text{if-I}}(t) = 2I_{2,1}e^{j(2\omega_L \pm \omega_s)t}.$$
(2)

Similarly, the output IF signal current of the subharmonic mixer Q is

$$i_{\text{if-Q}}(t) = \sum_{m=-\infty}^{m=+\infty} \sum_{n=-\infty}^{n=+\infty} \left[I_{m,n} e^{j(m\omega_L + n\omega_S)t} \times (1 - e^{j(m+n)\Delta\pi}) e^{(m+n)\Delta\psi} \right]$$

$$= 2I_{2,1} e^{j(2\omega_L \pm \omega_S)t} e^{j(2\pm 1)\Delta\psi}.$$
(3)

From (3), when $\omega_{if} = 2\omega_L - \omega_s$, the phase difference becomes to $\Delta\omega_{if} = \Delta\psi$. When all the circuits are ideal, then the output I-channel and Q-channel IF signals are orthogonal in phase and have equal amplitude.

The above analysis is performed based on ideal circuit components and structures. Now, let us assess the influence of amplitude and phase imbalances on the IQ mixer. If the LO hybrid coupler is not ideal, and the phase imbalance of the two output LO signals is defined as Δh_L , the output current of the I channel is as follows:

$$i_{\text{if-I}}(t) = 2I_{2,1}e^{j(2\omega_L \pm \omega_s)t}.$$
(4)

And the output current of the Q channel is

$$i_{\text{if-Q}}(t) = 2I_{2,1}e^{j(2\omega_L \pm \omega_s)t}e^{j(2\pm 1)\frac{\pi}{2}}e^{j2\Delta h_L}.$$
 (5)

Then the phase difference between the I and Q channels is

$$|\Delta\omega_{if}| = \left|\frac{\pi}{2} - 2\Delta h_L\right|. \tag{6}$$

Let us assume that there is an amplitude imbalance of ΔA_L dB between the two output ports of the LO hybrid coupler. When driving the mixer with a high-power LO signal, the mixer diode operates in a

switching state. In this state, its transconductance remains relatively constant even when the LO power experiences slight fluctuations. As a result, the amplitude of the IF signals in the I and Q channels remains nearly unchanged.

In addition, if the RF hybrid coupler is not ideal, the phase imbalance of the two output RF signals is Δh_s , and then the output current of the I channel is

$$i_{\text{if-I}}(t) = 2I_{2,1}e^{j(2\omega_L \pm \omega_s)t}. \tag{7}$$

And the output current of the Q channel is

$$i_{\text{if-Q}}(t) = 2I_{2,1}e^{j(2\omega_L \pm \omega_s)t}e^{j(2\pm 1)\frac{\pi}{2}}e^{j\Delta h_s}.$$
 (8)

Then the phase difference between the I and Q channels is

$$|\Delta\omega_{\rm if}| = \left|\frac{\pi}{2} - \Delta h_s\right|. \tag{9}$$

Assuming there is an amplitude imbalance of ΔA dB between the two output ports of the RF hybrid coupler. Since the amplitude of the IF current is linearly related to the amplitude of the RF voltage, the amplitude difference between the I-channel and Q-channel intermediate frequency signals is ΔA_s dB.

In summary, it can be concluded that both the amplitude and phase imbalances of the hybrid coupler affect the image suppression system of the IQ mixer. Specifically, when the amplitude imbalance between the two output ports of the RF hybrid coupler is ΔA_s dB, and the phase imbalance of the two output RF signals is Δh_s , while the amplitude imbalance between the two output ports of the LO hybrid coupler is ΔA_L dB, and the phase imbalance of the two output LO signals is Δh_L , then the amplitude imbalance between the two IF output ports of the I channel and Q channel is ΔA_s dB, and the phase imbalance is given by $|2\Delta h_L - \Delta h_s|$.

Based on the theoretical analysis, it is evident that for IQ mixers, implementing 3 dB hybrid couplers at both the LO and RF ports leads to improved isolation between the two subharmonic mixers and reduced standing waves at the RF and LO ports.

The 330 GHz IQ transceiver topology is illustrated in Figure 3. The entire circuit of the subharmonic mixer is fabricated on a quartz substrate. The RF signal is guided to the RF 3 dB hybrid coupler through a standard waveguide WR 2.8, where it is divided into two signals with the same amplitude and a 90° phase difference. Similarly, the LO driving signal reaches the LO 3 dB hybrid coupler through a standard waveguide WR 5.1, also splitting into two signals with the same amplitude and a 90° phase difference. The resulting IF signal generated by the subharmonic mixer can be output to the IF layer through the SMP connector, utilizing the high-pass characteristics of the waveguide structure. As the LO driving signal's frequency is only half that of the RF signal, it is below the cutoff frequency of the RF waveguide, preventing the LO energy from leaking to the RF port. The presence of an intermediate frequency filter further inhibits the escape of the driving signal from the intermediate frequency port, improving the energy utilization of the driving signal. Additionally, due to the useful RF signal's frequency range falling within the stopband of the LO low-pass filter, it can only be reflected and cannot pass through. As a result, the useful signal will not leak out from the LO and IF ports.

To ensure electrostatic protection, it is essential to prevent external static electricity from entering the circuit through the waveguide structure. However, the main concern is preventing static electricity from entering the circuit through the IF port of the subharmonic mixers. To address this, two static protection chips are strategically positioned at two IF ports. This placement effectively safeguards the mixer by preventing static electricity from entering and causing potential damage to the diodes.

2.2 330 GHz subharmonic mixers

The two 330 GHz subharmonic mixers employed in the transceiver module are identical. The circuit structure of the 330 GHz subharmonic mixer is illustrated in Figure 3. The RF input signal and local oscillator signal are fed through WR 2.8 and WR 5.1 standard waveguides, respectively. Subsequently, a waveguide microstrip transition structure converts the TE10 mode to a quasi TEM mode for suspended microstrip transmission.

When designing a circuit involving mixing frequencies, it is crucial to establish a comprehensive signal grounding circuit for both the mixing frequency and the generated frequency. To achieve this, the

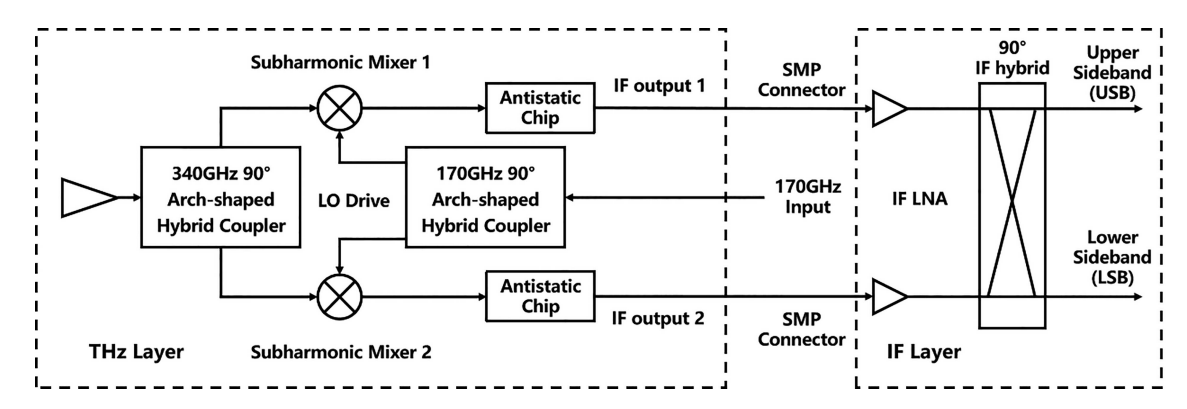


Figure 3 The topology of the 330 GHz vertical interconnect IQ transceiver.

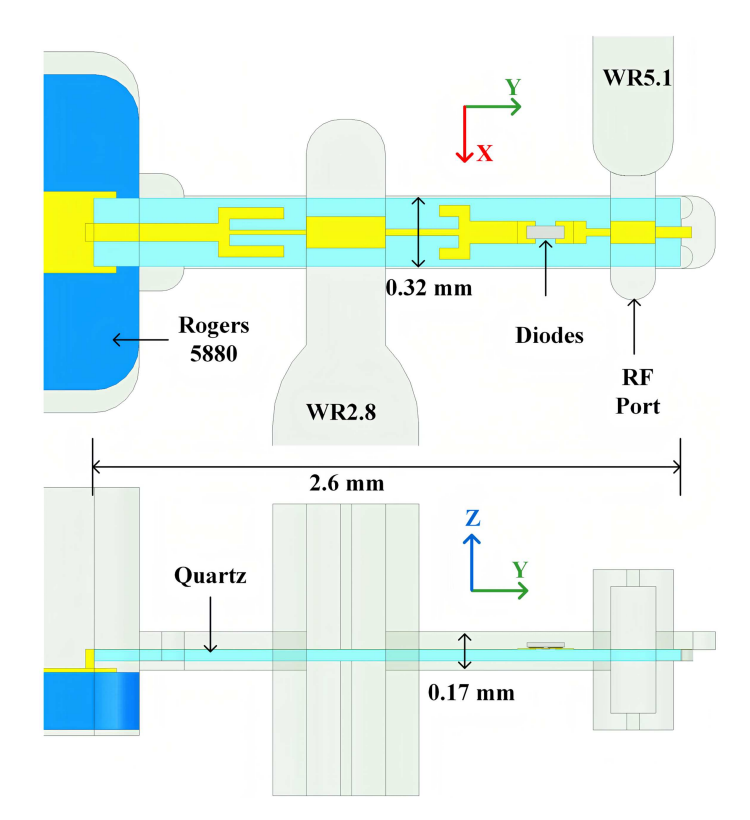


Figure 4 (Color online) The circuit structure of the 330 GHz subharmonic mixer.

microstrip circuit is electrically connected to the metal cavity across the RF waveguide. This connection serves the purpose of IF/DC grounding and effectively short-circuits the local oscillator signal. To prevent the leakage of the local oscillator signal to the RF port and limit the leakage of the intermediate frequency signal through the waveguide, the high-pass characteristic of the waveguide is utilized to cut off the transmission of the local oscillator signal within the RF waveguide. In Figure 4, the two open branches are designed specifically to block the flow of RF or LO signals, while maximizing the energy loading onto the diode. This arrangement ensures efficient operation and minimizes signal interference during the mixing process [20].

The 50 μ m-thick quartz circuit is embedded within an air channel measuring 320 μ m in width and 170 μ m in height, forming a suspended microstrip structure that ensures low transmission loss. Symmetrical folded open-circuit stubs are utilized as RF and LO filters, enabling the quartz substrate to be shortened to a compact length of just 2.6 mm. This miniaturized design significantly facilitates the processing and assembly of quartz circuits. To further reduce the overall height, the RF input waveguide is modified to function not only as an additional matching branch of the RF matching network but also to decrease the distance between the microstrip short and the diode chip.

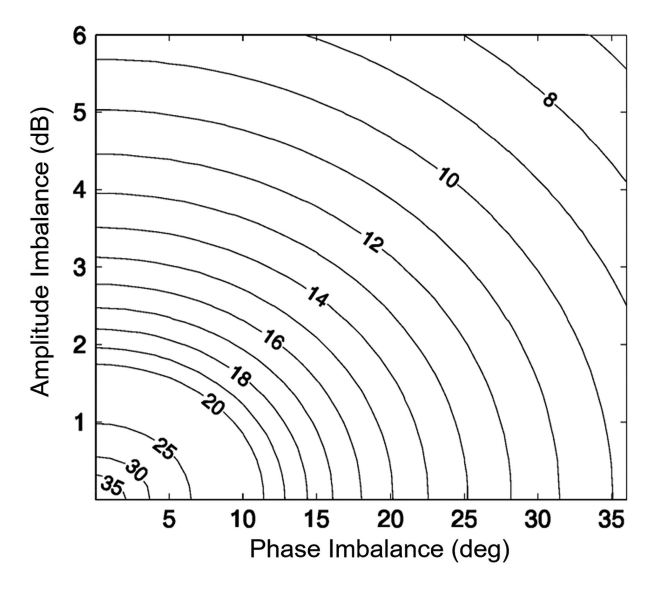


Figure 5 The relationship between IRR and the amplitude and phase imbalance.

At room temperature, the mixer achieves an SSB conversion loss of less than 10 dB across the 300–355 GHz frequency range with 3 mW of LO power at 164.5 GHz. A minimum SSB CL of 8 dB is obtained at 330 GHz.

2.3 Compact arch-shaped hybrid couplers

The RF and LO hybrid coupler adopts a branch waveguide coupler structure, and its isolation port requires a matching network. However, if the terminals cannot be fully matched, it can introduce noise from the environment into the mixer, leading to increased receiver noise. When noise enters the isolation port and undergoes frequency conversion, the upper and lower sidebands of the IF port will reverse compared to the RF signal entering the input port, resulting in poor quality of the IF signal. Regarding the LO hybrid coupler feeding, as there are no even mode terminals in the RF feeding structure, the noise generated at the RF port of the mixer may leak into another mixer, leading to an overall increase in transceiver noise. Poor RF matching of the mixer can cause ripple due to RF standing waves, which will affect receiver performance.

The image rejection ratio (IRR) is a critical performance indicator for IQ mixers. Therefore, it is essential to analyze the impact of amplitude and phase imbalances between the two IF output signals on image suppression performance. The IRR in an IQ mixer is a function of amplitude imbalance and phase imbalance, and it is defined as

$$IRR = \sqrt{\frac{(1+\delta+\cos\alpha)^2 + \sin^2\alpha}{(1+\delta-\cos\alpha)^2 + \sin^2\alpha}}.$$
 (10)

In the equation, δ represents the difference between the output power of the I-channel and Q-channel signals, which is also defined as the amplitude imbalance. Additionally, α signifies the absolute difference between the phase difference and 90° between the two IF signals, known as phase imbalance. The relationship between the IRR and the amplitude and phase imbalance is depicted in Figure 5. By measuring the amplitude and phase imbalance of the I and Q channels, it becomes possible to calculate the approximate IRR of the developed mixer. In the development of an IQ mixer, achieving image rejection performance better than 20 dBc is typically desired. To attain this level of performance, based on the relationship presented in Figure 6, the amplitude imbalance needs to be less than 2 dB, and the phase imbalance should be less than 10°.

To achieve a compact size while maintaining good amplitude and phase imbalance, a modified arch-shaped hybrid coupler is investigated. This design involves cutting four round grooves at the four corners of the branch walls, forming an arch-shaped branch. The gradient structure loaded with electric field perturbations helps reduce the impact of discontinuities on circuit performance, leading to improved amplitude and phase imbalance performance [21].

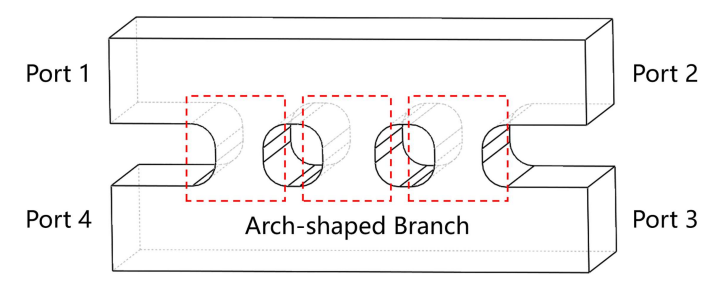


Figure 6 (Color online) The relationship between mirror frequency suppression level and the amplitude and phase imbalance.

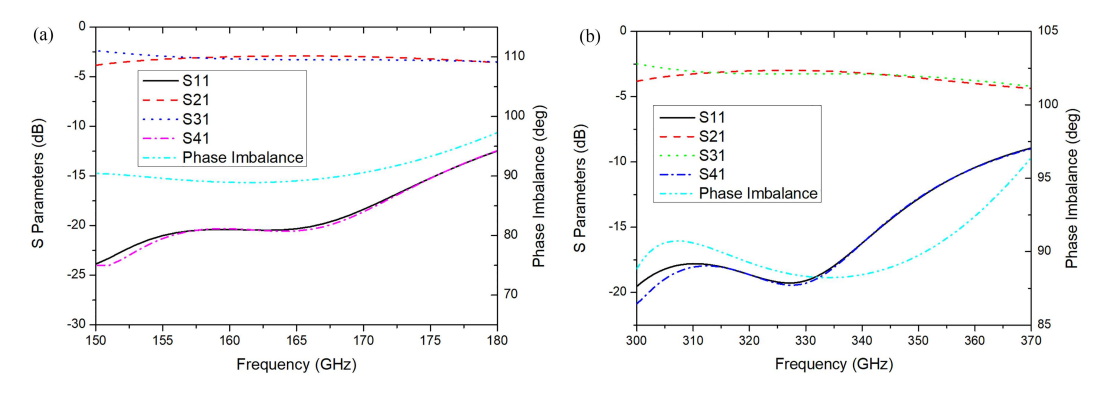


Figure 7 (Color online) Simulated results from the 3-arch-shaped-branch hybrid couplers. (a) 165 GHz LO hybrid coupler. The power and phase balance are better than 0.35 dB and 5°, respectively. (b) 330 GHz RF hybrid coupler. During 305–360 GHz, the power and phase balance are better than 0.3 dB and 3°, respectively.

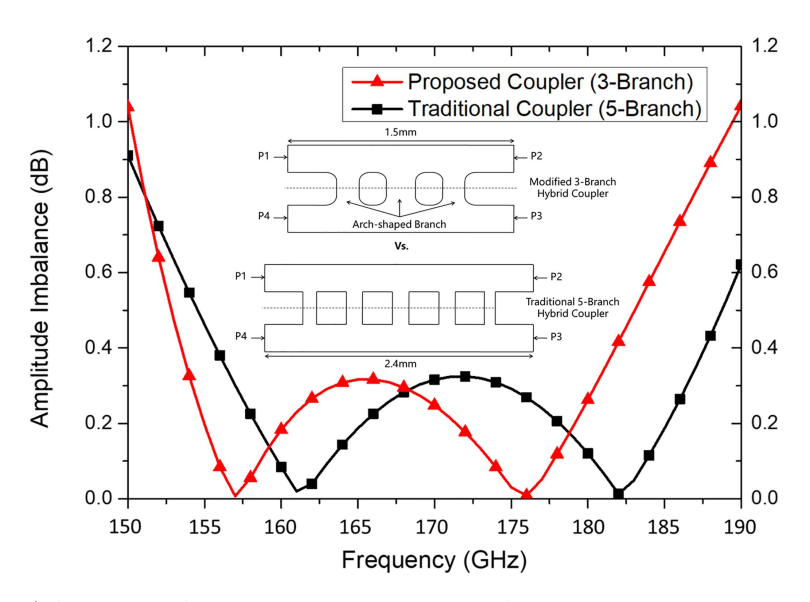


Figure 8 (Color online) Comparison of simulation results between modified 3-branch hybrid coupler and traditional 5-branch hybrid coupler.

After optimization, the LO and RF hybrid coupler structure is shown in Figure 6. The hybrid coupler incorporates three arch-shaped branches, and the performance of the 165 and 330 GHz hybrid couplers is depicted in Figure 7. The operation bandwidth widens as the number of branches increases [22]. Comparing the traditional 5-branch hybrid coupler with the 3-arch-shaped modified hybrid coupler, as shown in Figure 8, it becomes apparent that the size of the proposed compact 3-branch hybrid branch exhibits 60% less than the traditional 5-branch hybrid structure, while maintaining almost the same performance.

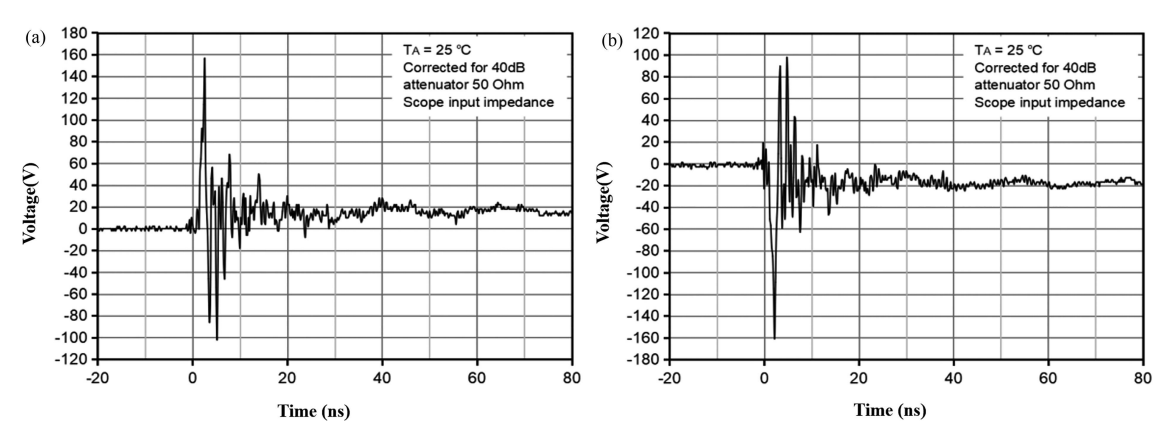


Figure 9 The ESD contact test of ± 8 kV. (a) + 8 kV clamping waveform; (b) - 8 kV clamping waveform.

2.4 Antistatic chip

Electrostatic discharge (ESD) is an age-old natural phenomenon involving the transfer of charges when two objects with different electrostatic potentials come close or make contact. While static electricity has minimal impact on the human body, it can significantly damage semiconductor integrated circuits with withstand voltages ranging from a few to tens of volts. ESD can lead to the breakthrough of these integrated circuits, causing large transient currents. To prevent circuit damage, companies like Virginia Diodes Inc. (VDI) or ACST GmbH (ACST) emphasize ESD protection measures in their product data sheets.

In actual testing processes, testers may wear an electrostatic bracelet or add a collimator to the IF port of the mixer to prevent ESD. However, these measures can increase operational complexity for testers and result in larger circuit volumes and increased circuit loss.

In this paper, a 4-line, uni-directional, ultra-low capacitance system-level transient voltage suppressors chip (TVS) fabricated by using 0.5 μm bipolar CMOS DMOS (BCD) technology is utilized to safeguard 330 GHz subharmonic mixers from ESD stress. This TVS chip consists of one pair of ultra-low capacitance steering diode strings and a low leakage clamp with high holding snap-back characteristics. Its purpose is to protect the power supply line and ensure robust latch-up immunity. The foorprint of the newly-added TVS chip is about 400 $\mu m \times 400~\mu m$. Its measurement results are depicted in Figure 9. Apart from the GND pin, all other pins are equivalent. Therefore, a single TVS chip can fulfill the ESD protection requirements of two subharmonic mixers.

This chip was originally developed for system-level ESD protection in high-speed data ports (e.g., USB $3.0, \mathrm{HDMI}$) [23]. Its key feature is the use of low-capacitance steering diodes to reduce both differential-mode and common-mode capacitance of the entire chip. This approach ensures that the fundamental frequency performance remains unaffected while reducing packet loss, and at the same time provides robust ESD protection (air discharge: $8 \mathrm{\ kV}$ @ IEC 61000-4-2 Level 4).

In the design described in this work, the chip area was slightly increased, and a higher-resistivity substrate along with lower-dose ion implantation was adopted. Meanwhile, minor modifications were made to the pins to facilitate efficient interconnection between the two subharmonic mixers in the IQ transceiver. As a result, the measured ESD performance was improved to 10 kV, while the differential-and common-mode capacitance remained nearly unchanged.

2.5 Transceiver structure

The whole transceiver structure exploded diagram is shown in Figure 10. The IF circuit includes an IF hybrid and an IF low-noise amplifier. The entire module is encapsulated within a cavity module, connected to the terahertz circuit via SMP connectors. This IF circuit connects through SMP connectors, making it easy to assemble and disassemble. This allows for separate testing of the IF circuit and terahertz circuit performance, addressing the difficulties traditionally encountered in integrated circuit testing. It also enables tuning to find the overall circuit's optimal working condition.

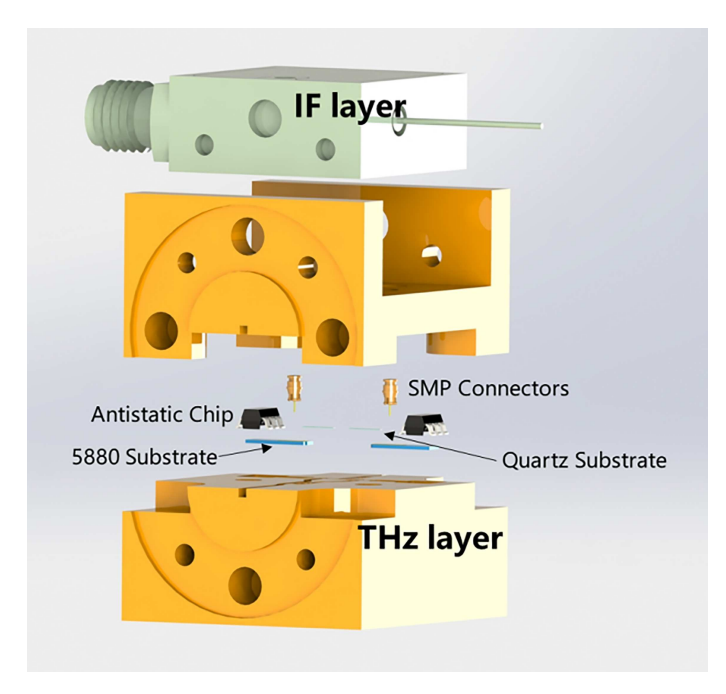


Figure 10 (Color online) The whole transceiver structure exploded diagram.

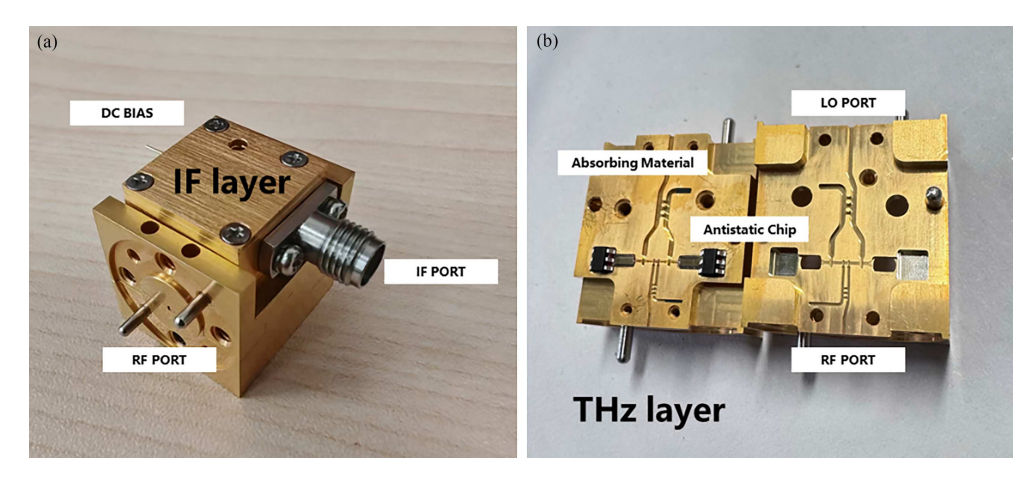


Figure 11 (Color online) The assembled 330 GHz anti-static compact vertical interconnect IQ transceiver. (a) The whole block; (b) the inner block.

3 Measurements and results

The 330 GHz IQ transceiver is fabricated using CNC precision machining technology, and the assembled 330 GHz anti-static compact vertical interconnect IQ transceiver is depicted in Figure 11. In consideration of circuit miniaturization, MXene absorbing material is strategically placed at the end of the isolation ports of the 330 and 165 GHz hybrid couplers as the matching load [24]. This enhances the performance of the hybrid couplers.

For transceiver measurements, both a 330 GHz RF signal and a 165 GHz LO drive signal are required. The IF circuits can be measured separately due to the SMP connections. With the LO frequency set at 165 GHz and a driving power of 10 mW, the output power effectively drives both two subharmonic mixers. Additionally, the measurement results of the frequency conversion loss and IRR of the IQ transceiver, as shown in Figure 12. Within the RF frequency range of 305–355 GHz, the frequency conversion loss of the mixer remains below 10 dB, the amplitude imbalance is less than 1.6 dB, and the phase imbalance is less than 7.6°.

The comparison among the proposed terahertz IQ transceivers is presented in Table 1. These reference studies are founded on solid-state circuits. The proposed IQ transceiver, utilizing the modified 330 GHz

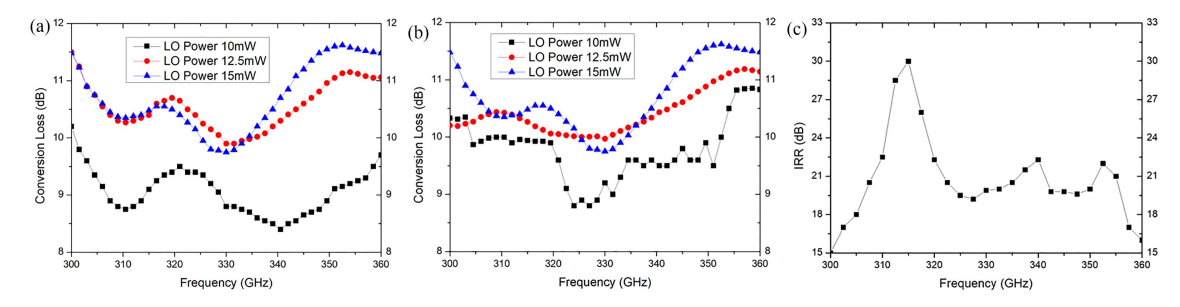


Figure 12 (Color online) The measurement results of the 330 GHz IQ transceiver. (a) The conversion loss of the I channel subharmonic mixer; (b) the conversion loss of the Q channel subharmonic mixer; (c) IRR of the IQ transceiver.

Table 1 Companion of anticient 112 by transcervers.							
	Ref.	Frequency (GHz)	SSB CL (dB)	IRR (dB)	Size	Integrate IF circuits or not	Electrostatic prevention or not
	[13]	320-360	10-11	7.2 - 24.1	N/A	No	No
	[14]	320-360	9	>15	$40~\mathrm{mm}\times40~\mathrm{mm}\times20~\mathrm{mm}$	No	No
	[15]	80-120	12 - 18	8-43	$40~\mathrm{mm}\times30~\mathrm{mm}\times20~\mathrm{mm}$	No	No
	[16]	75 - 110	6-17	>10	$50~\mathrm{mm}\times25~\mathrm{mm}\times20~\mathrm{mm}$	Yes	No
	[17]	210 – 230	6.8 - 7.5	$27@220~\mathrm{GHz}$	$45~\mathrm{mm}\times30~\mathrm{mm}\!\times\!20~\mathrm{mm}$	No	No
	This work	305-355	8-10	>18	20 mm × 20 mm × 22 mm	Ves	Ves

Table 1 Comparison of different THz IQ transceivers.

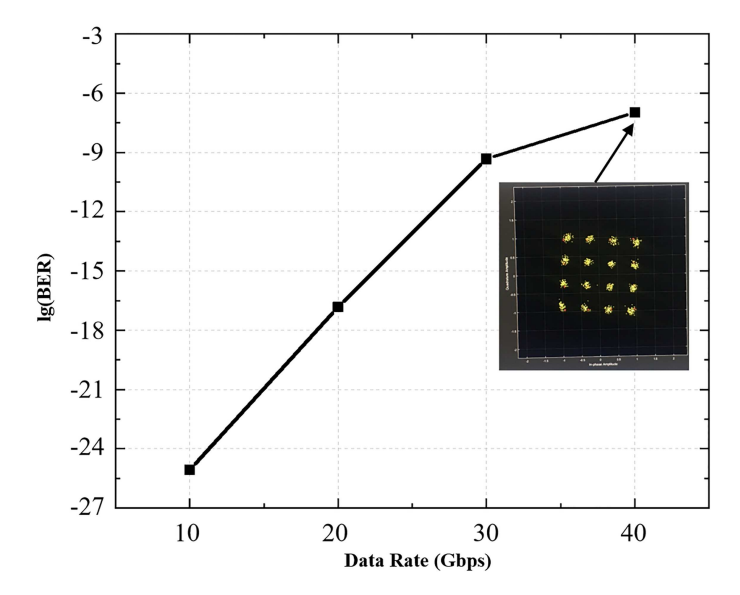


Figure 13 (Color online) Measurement results of BER versus different code rates. The inset shows the constellation diagram for a 40 Gbps communication rate.

subharmonic mixer and compact arch-shaped hybrid couplers, has achieved impressive performance with a typical conversion loss of 9 dB and an IRR of 18 dB. Moreover, it boasts a compact size of 20 mm \times 20 mm \times 22 mm and successfully integrates IF circuits in a single block. Additionally, the IQ transceiver incorporates an antistatic chip to ensure effective protection of the diodes.

To evaluate its performance in high-speed communication systems, a high-speed communication test platform was established. The measurement results of BER versus different code rates are shown in Figure 13. At the transmitter side, baseband signals were generated by an arbitrary waveform generator. To achieve high-speed data transmission, the IF modulation signal employed 16QAM modulation with a roll-off factor set to 0.15. After mixing with a 330 GHz signal, the baseband data were fed into the IQ transceiver developed in this work. On the receiver side, the demodulated signals were captured using a high-speed oscilloscope and subsequently transferred to a PC for processing.

For QAM modulation, the constellation diagram provides a visual method to assess data transmission quality; the closer the received signals cluster around the constellation points, the better the signal

quality. During the experiment, the baseband signal bandwidth was set to 10 GHz, and the resulting constellation diagrams were observed. As shown in Figure 13, even at a transmission rate of 40 Gbps, the 16 constellation points remained well clustered, indicating that the developed 330 GHz IQ transceiver exhibits excellent performance.

4 Conclusion

This article focuses on the study of terahertz IQ mixers, including selecting the most suitable implementation for the terahertz frequency band, analyzing key factors affecting IQ mixer performance, and proposing a 330 GHz antistatic compact vertical interconnect IQ transceiver. To enhance the overall performance of the transceiver, the research explores a modified 330 GHz subharmonic mixer and compact arch-shaped hybrid couplers. Utilizing SMP connectors, the transceiver achieves low-loss multi-layer circuit interconnection in the vertical direction, reducing volume and circuit losses in the front-end.

Additionally, to protect the mixer from electrostatic discharge, an anti-static chip is integrated into the circuit, ensuring the reliable operation of the subharmonic mixers. The 330 GHz IQ transceiver achieves a conversion loss as low as 9 dB and an IRR of 18 dB. Owing to its high performance, the transceiver can be readily integrated into high-speed communication systems, serving as a key component for achieving 40 Gbps data rates in future 6G applications.

Acknowledgements This work was supported by Mobile Information Networks National Science and Technology Major Project (Grant No. 2025ZD1303000), in part by Natural Science Foundation of Sichuan (Grant No. 2024YFHZ0090), Shenzhen Science and Technology R&D Funding (Grant Nos. KJZD20231023094659001, KJZD20240903100200001, RCJC20221008092806008, 7BJB25010A), and Natural Science Foundation of Zhejiang (Grant No. LD25FO40007).

References

- 1 Tong W, Zhu P Y. 6G: the Next Horizon: From Connected People and Things to Connected Intelligence. Cambridge: Cambridge University Press, 2021. 1–5
- $2\,\,$ Tonouchi M. Cutting-edge terahertz technology. Nat Photon, 2007, 1: 97–105
- $3\,\,$ Graham-Rowe D. Terahertz takes to the stage. Nat Photonics, 2027, 1: 75–77
- 4 Jansen C, Wietzke S, Peters O, et al. Terahertz imaging: applications and perspectives. Appl Opt, 2010, 49: 48–57
- 5~ Ho L, Pepper M, Taday P. Signatures and fingerprints. Nat Photon, 2008, 2: 541-543
- 6 Pickwell E, Wallace V P. Biomedical applications of terahertz technology. J Phys D-Appl Phys, 2006, 39: R301–R310
- 7 Liu K, Feng Y, Han C, et al. High-speed 0.22 THz communication system with 84 Gbps for real-time uncompressed 8K video transmission of live events. Nat Commun, 2024, 15: 8037
- 8 Wu L S. Terahertz communication systems for real-world video transmission. Nat Rev Electr Eng, 2024, 1: 638
- 9 Niu Z, Zhang B, Zhang Y, et al. Solid-state terahertz circuits for 6G: a review. Chin J Elect, 2025, 34: 373–400
- 10 Ho T H, Chung S J. Design and measurement of a Doppler radar with new quadrature hybrid mixer for vehicle applications. IEEE Trans Microwave Theory Tech, 2010, 58: 1–8
- 11 Khudchenko A, Hesper R, Baryshev A M, et al. Modular 2SB SIS receiver for 600–720 GHz: performance and characterization methods. IEEE Trans Terahertz Sci Technol, 2017, 7: 2–9
- 12 Siddiqua M. Design & analysis of an X-Band QPSK modulator using direct carrier modulation technique. In: Proceedings of IEEE International Multitopic Conference, 2006. 106–110
- 13 Thomas B, Rea S, Moyna B, et al. A 320–360 GHz subharmonically pumped image rejection mixer using planar Schottky diodes. IEEE Microw Wireless Compon Lett, 2009, 19: 101–103
- 14 Sobis P J, Emrich A, Stake J. A low VSWR 2SB Schottky receiver. IEEE Trans THz Sci Technol, 2011, 1: 403-411
- 15 Gawande R, Reeves R, Samoska L, et al. W-band IQ sub-harmonic mixers with low LO power for cryogenic operation in large arrays. In: Proceedings of the 9th European Microwave Integrated Circuit Conference, 2014. 301–304
- 16 Monasterio D, Jarufe C, Gallardo D, et al. A compact sideband separating downconverter with excellent return loss and good conversion gain for the W band. IEEE Trans THz Sci Technol, 2019, 9: 572–580
- 17 He Y, Liu G, Liu J, et al. A 220 GHz orthogonal modulator based on subharmonic mixers using anti-paralleled Schottky diodes. Chin J Electron, 2022, 31: 562–568
- 18 Akyildiz I F, Han C, Hu Z, et al. Terahertz band communication: an old problem revisited and research directions for the next decade. IEEE Trans Commun, 2022, 70: 4250–4285
- 19 Lin W H, Yang H Y, Tsai J H, et al. 1024-QAM high image rejection E-band sub-harmonic IQ modulator and transmitter in 65-nm CMOS process. IEEE Trans Microwave Theor Techn, 2013, 61: 3974-3985
- 20 Liu Y, Niu Z, Zhang B, et al. A high-performance 330-GHz subharmonic mixer using Schottky diodes. IEEE Microw Wireless Compon Lett, 2022, 32: 571–574
- 21 Rashid H, Desmaris V, Belitsky V, et al. Design of wideband waveguide hybrid with ultra-low amplitude imbalance. IEEE Trans THz Sci Technol, 2016, 6: 83–90
- 22 Reed J. The multiple branch waveguide coupler. IEEE Trans MicrowTheory Techn, 1958, Mtt-6: 398–403
- 23 Qi Z, Qiao M, Wei J Q, et al. Novel multifunctional transient voltage suppressor technology for modular EOS/ESD protection circuit designs. In: Proceedings of the 35th International Symposium on Power Semiconductor Devices & ICs, Hong Kong, 2023. 72–75
- 24 Zhao T Z, Xie P Y, Wan H J, et al. Ultrathin MXene assemblies approach the intrinsic absorption limit in the 0.5–10 THz band. Nat Photonics, 2023, 17: 622–628